Nano Research 2018, 11(8): 4265–4277
https://doi.org/10.1007/s12274-018-2013-0
Research Article
ISSN 1998-0124
CN 11-5974/O4

Natural polypeptides treat pollution complex: Moisture-resistant multi-functional protein nanofabrics for sustainable air filtration

Huafeng Tian[1], Xuewei Fu[2], Min Zheng[2], Yu Wang[2] (✉), Yichao Li[3], Aimin Xiang[1], and Wei-Hong Zhong[2] (✉)

[1] *School of Material and Mechanical Engineering, Beijing Technology and Business University, Beijing 100048, China*
[2] *School of Mechanical and Materials Engineering, Washington State University, Pullman, Washington 99164, USA*
[3] *School of Aerospace Engineering, Huazhong University of Science and Technology, Wuhan 430074, China*

Received: 12 December 2017
Revised: 17 January 2018
Accepted: 30 January 2018

KEYWORDS
zein nanofabric, multi-functional air-filtration, water-resistant, protein air-filter

ABSTRACT

Development of "green" multi-functional air filters with features such as excellent filtration efficiency, eco-friendliness, and environmental stability are critically required to address the increasing concerns of polluted air. Natural proteins, such as soy protein and gelatin, are attractive candidates as multi-functional air-filtration materials owing to the rich functional groups; however, these bio-materials are vulnerable to moisture, which limits their broad application in practice. In this work, a hydrophobic protein of zein derived from abundant corn is modified for the first time to produce high-performance nanofilters via electrospinning. The zein nanofabrics are fabricated with the aid of a non-toxic solvent and co-electrospinning agent, poly(ethylene oxide). The results reveal that the zein-based nanofabrics show high efficiency for the simultaneous removal of particulate matters of different sizes ranging from 0.1 to 10 μm (> 99.5%) and certain gaseous toxic chemicals (> 70%). In addition, the zein nanofabrics show excellent moisture-resistance and good adhesion to the cellulose paper towel used as the air-filter substrate. This study demonstrates that nanofabrics based on hydrophobic natural proteins such as zein are promising materials for developing multi-functional "green" air filters.

1 Introduction

Air pollution due to numerous pollutants such as particulate matter (PM) of various sizes, toxic chemical gases, and biological hazards has become one of the most critical concerns very relevant to ecological environment and public health [1, 2]. Particulate pollutants are the primary constituents causing bad air quality and they severely impact the human body. PM can be classified into several categories based on the particulate size, e.g., $PM_{2.5}$ of particulate sizes below 2.5 μm that can penetrate into human lungs,

Address correspondence to Yu Wang, yu.wang3@wsu.edu; Wei-Hong Zhong, katie_zhong@wsu.edu

$PM_{2.5–10}$ of sizes between 2.5 and 10 μm [3]. In addition to PM pollutants, chemical gases that are released from industries and human activities are also commonly found in polluted air; these include, formaldehyde (HCHO), carbon monoxide (CO), various sulfur compounds, and other volatile organic compounds (VOCs) [4, 5]. The complicated constituents of polluted air do not only pose risks to human health, but also cause other issues such as environmental hazards from photochemical reactions of the VOCs [6]. At the same time, a large number of particulates and chemicals can undergo various interactions to form complex pollutant derivatives, posing increased threats to humans and other organisms [7]. Therefore, there is an increasing demand for high-performance air filtration materials enabling the simultaneous capture of PM pollutants and gaseous chemical hazards.

Currently available commercial air filtration materials are typically fabricated in nonwoven forms with randomly interconnected micro-/nano-sized fibers that are primarily derived from synthetic polymers such as polyethylene (PE), polypropylene (PP), and glass fibers [8]. Such porous and fibrous air filters effectively capture particulates owing to the size effect [9]; however, the inert surface and inadequate surface area of the conventional air filters limit their capability to capture gaseous chemical substances. Thus, a high loading of high-surface area additives such as activated carbon is usually employed to absorb small chemical molecules. In fact, at present, to achieve high-performance filtration of both particulates and gaseous chemicals, one has to combine multiple components in the filter, e.g., conventional fibrous mats with activated carbon. These combinations induce excessive materials cost and processing, and more serious effects are the increases in air resistance, and thus, extra energy consumption [10]. In addition, these synthetically produced air filters based on petroleum are difficult to degrade, and they release pollutants during their production processes as well as cause secondary pollution after disposal [11, 12]. Therefore, the development of multi-functional air filters comprising "green" materials that can effectively remove both particulate pollutants and toxic chemical gases is a very attractive solution to resolve the aforementioned issues [13].

In previous studies, protein-based nanofibers prepared by electrospinning, including soy protein, silk, and gelatin, have been used as "green" and multi-functional air filters, with excellent removal efficiency for PM pollutants and certain toxic chemical gases [3, 10, 11, 14]. Such high performance of protein-based air filters has been realized for the following reasons: First, the electrospun nanofibers [10, 15–18] possess large specific surface area and porous structures, which allow the flow of air and facilitate stronger filter-pollutant interactions compared to micro-fiber-based filters. Second, proteins possess abundant functional groups derived from 20 amino acids [19, 20], which can potentially facilitate strong interactions with different types of pollutants such as toxic chemical gases and particulates of sizes much smaller than the pore sizes of the air filters. However, the mechanical weakness and moisture sensitivity of these natural proteins have severely limited their broad application. In our recently reported work [21], we demonstrated that cross-linked gelatin protein nanofibers show improved water-resistance and good removal efficiency for both particulates and chemical gases in a highly humid environment. As another strategy for addressing the issue of moisture sensitivity, we propose a cost-effective approach for fabricating protein-based air filters by applying zein, a hydrophobic protein with excellent moisture resistance. As a prolamine, zein is more hydrophobic than other proteins owing to a high percentage of non-polar amino acid residues including proline, leucine, alanine, and glutamine [22–24]. Specifically, zein has greater than 50% hydrophobic domains on the surface [25]. To improve the processability and mechanical properties of zein nanofabrics, a blending polymer, polyethylene oxide (PEO), is employed. Compared to many widely used blending polymers, such as polyurethane [26, 27], acrylonitrile-butadiene-styrene [28], poly (acrylic acid) [29], polydimethylsiloxane [30], epoxy [31, 32], poly(L-lactide) [33], and poly(vinyl alcohol) [34], PEO is non-toxic and very compatible with the zein precursor solution. As a result, we successfully fabricated a high-performance zein-based protein nanofilter with good mechanical properties, excellent water-resistance, and high removal efficiency for pollutants (particulates and gaseous chemicals) in both dry and humid conditions, as well as good adhesion to paper towel used as the substrate.

2 Experimental

2.1 Materials

Zein was purchased from Shanghai Yuanye Bio-technology

Co., Ltd (purity, 92%). PEO with a molecular weight of 600,000 g·mol^{-1} was obtained from Sigma-Aldrich. Acetic acid (99.9%) was purchased from J.T. Baker (Center Valley, PA, USA). Other chemicals were obtained from Sigma-Aldrich and used as received.

2.2 Preparation of zein nanofabrics

The zein solution with a solid content of 7 wt.% was prepared by dissolving zein powder in acetic acid/deionized (DI) water (weight ratio, 80:20) at room temperature. The mixture was stirred for ~ 1 h to achieve a homogeneous yellow solution. At the same time, a PEO solution was prepared in the same solvent and mixed with the zein solution according to varying loadings of PEO, e.g., 4 wt.%, 7 wt.%, 15 wt.%, and 25 wt.% with respect to the total solid content of zein and PEO to obtain the precursor solution for electrospinning. The final concentration of the precursor solution was set to 7 wt.%, except for the 25 wt.% PEO loading sample which was prepared at a concentration of 4.5 wt.% owing to its high viscosity. The mixed solution was loaded into a syringe (Monojet Kendall) with a 21-gauge blunt-tip needle. A voltage in the range of 16–21 kV was applied for electrospinning and it was controlled by a high-voltage power source (ES50P-5W, Gamma High Voltage Research). A monoinject syringe pump (KD Scientific, KDS-100) was used to pump the zein solution. The paper towel substrate was fixed on a grounded commercial copper mesh with a wire diameter of 0.011 inch and mesh pore size of 1 mm × 1 mm to collect the nanofibers onto the paper towel. The distance between the needle and the sample collector was fixed at 10 cm, and an average flow rate of 0.6 mL·h^{-1} was utilized. Moreover, the position of the needle (horizontal and vertical) was adjusted continuously during electrospinning to achieve a uniform fiber mat with a controlled nanofiber diameter and different areal densities.

2.3 Characterization and air-filtration testing

Scanning electron microscopy (SEM, FEI SEM Quanta 200F) was utilized to investigate the morphological characteristics of the filter mats. The average fiber diameter and pore size were statistically analyzed by Image-Pro Plus software. Fourier transform infrared (FTIR) spectroscopy (Thermofisher iS10) was employed to study the functional groups as well as the interactions between the nanofiber and pollutants. The mechanical performance of the nanofabrics was evaluated on a universal testing machine (Instron, 5565A) and the stress-strain curves were obtained with a tensile rate of 5 mm·min^{-1}. The polluted air samples produced by burning joss sticks were diluted in a plastic gasbag to a hazardous and measurable level for the analyzer because of the very high initial pollutant concentration. A particle counter (CEM, DT-9881) with chemical sensors for CO and HCHO was used to determine the concentrations of PM (different particle sizes from 0.3 to 10 μm) and toxic chemicals (HCHO and CO) in the polluted air samples. To evaluate the filtration performance in humid condition, a humidifier was used to generate moisture in the gasbag and the relative humidity (RH) was recorded by the particle counter. A circular filter sample with a diameter of 37 mm was placed in a custom-made sample holder to perform air-filtration testing. The downstream air of the filter was collected in a clean vacuum gasbag. Similar measurements were conducted for the collected filtered air, downstream of the filter. The air-filtration testing procedures have been described in detail in our previous report [14].

3 Results and discussion

Figure 1 illustrates the schematic of the preparation of flexible and water-resistant zein-based nanofabrics for air filtration. As already mentioned, sensitivity to humidity and mechanical brittleness are the critical drawbacks preventing the practical application of protein-based nano-air-filters, which was encountered in previously reported protein-based air filters. In this work, we focused on a different protein, zein, which comprises ca. 18 different amino acids [23], and more importantly, is highly hydrophobic to exhibit good water-resistance property. The zein protein was first denatured in a mixture of acetic acid (HAc) and DI water (weight ratio of 8:2) to expose the buried functional groups. To alleviate the brittleness of the protein and adjust the morphology of the nanofiber, a medium molecular weight polymer, PEO (M_W = 600,000 g·mol^{-1}) was blended with the denatured-zein solution. The

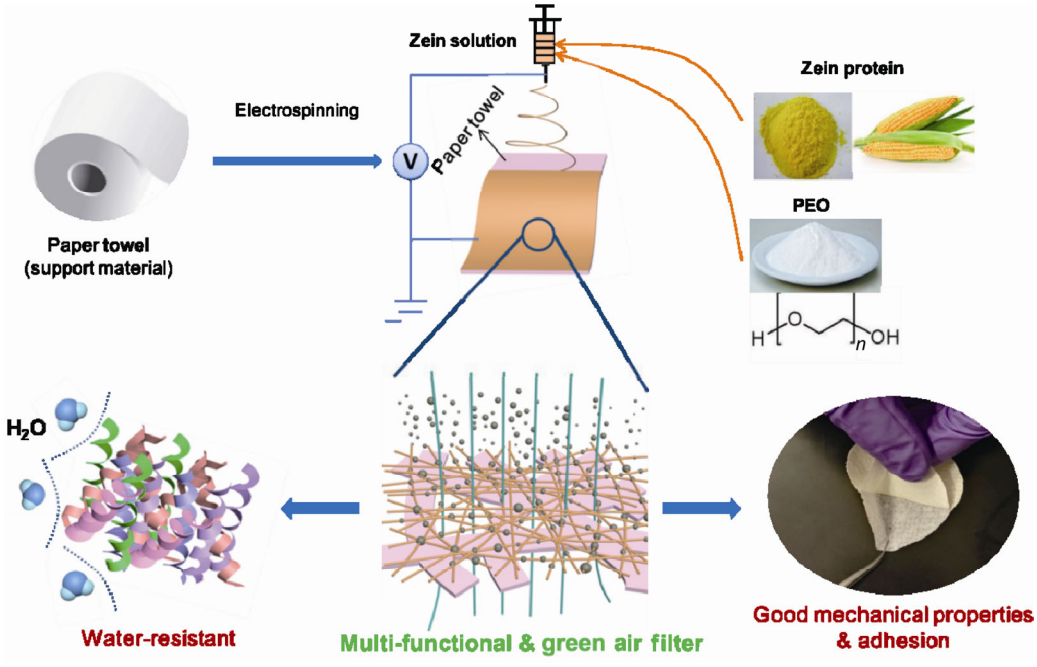

Figure 1 Schematic showing the fabrication of multi-functional green air nano-filter based on hydrophobic and flexible zein-based nanofabric (for details, see the text).

zein nanofabrics were deposited by electrospinning the mixed solution onto a paper towel sample mainly composed of cellulose microfibers, which provides mechanical support as well as some air filtration performance owing to its porous structure, which was specifically investigated in our previous work [35]. It was also found that the zein nanofabrics interact strongly with the paper towel substrate owing to hydrogen bonding, as will be discussed later, which is significantly beneficial in terms of the conformability, processing, and overall mechanical properties of the filter.

We first investigated the morphologies of the zein-based nanofibers with varying loadings of the protein, and the results are shown in Fig. 2. As shown, the morphological characteristics of the protein nanofabric, such as the fiber shape, fiber diameter, and pore size, are generally affected by the loading of PEO. In specific, neat zein protein without the blending agent PEO in the HAc/DI solvent could not be electrospun into nanofibers, and only beads or particles were observed on the substrate, as shown in Fig. 2(a). However, as shown in Figs. 2(b)–2(e), the introduction of PEO dramatically enhanced the electrospinning ability of zein solutions with deposits of randomly oriented nanofibers on the paper towel substrate. More specifically, the loading of PEO in the blends of zein/PEO played a critical role in controlling the morphology of the nanofibers. As is clear from the SEM images, the fiber shape changed significantly with the PEO loading. In case of lower PEO loading, such as for the samples with a high zein loading of 96% and 93% (Figs. 2(b) and 2(c)), ribbon-like nanofibers can be observed due to the high volatility of the HAc solvent, which is consistent with the results of other reported works using aqueous ethanol solution as the solvent [36–38]. However, with higher loading of PEO, as shown in Figs. 2(d) and 2(e), the nanofibers present a round shape with some small diameter intervals in the nanofibers, which may be ascribed to the increased attractive force under the high-voltage field with increased loading of PEO.

In addition to the fiber shape, the fiber diameter and pore size distribution were also affected by PEO loading and were statistically analyzed by Image-Pro Plus (see Fig. S1 in the Electronic Supplementary Material (ESM)). The results are summarized in Fig. 2(f). As illustrated, the diameter of the nanofibers slightly increases from ca. 340 nm to ca. 440 nm with an increase in the loading of zein from 75% to 85%, followed by a continuous decrease in the nanofiber diameter with further increase in the protein loading, e.g., ca. 230 nm

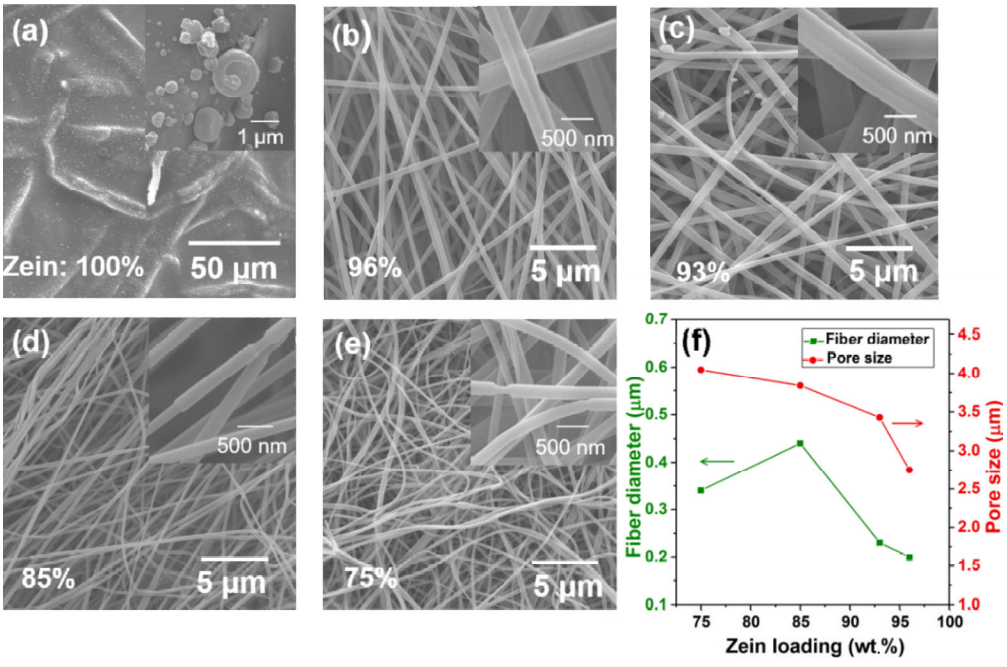

Figure 2 Morphological studies on zein-based nanofibers with varying loadings of zein protein. (a)–(e) SEM images of zein nanofibers with varying protein contents: 100 wt.%, 96 wt.%, 93 wt.%, 85 wt.%, and 75 wt.%, respectively. (f) The nanofiber diameter and pore size of the zein nanofabrics versus the loading of zein.

for 93% zein loading and ca. 200 nm for 96% zein loading. For the case of nanofibers electrospun from a solution with 75% zein, as the viscosity of the precursor solution was too high to electrospin, a solution with lower solid concentration (4.5%) was used, which resulted in smaller nanofiber diameter than the case of nanofibers electrospun from a solution with 85% zein. In addition to the nanofiber diameter, the pore size of the protein nanofibers also depended significantly on the PEO loading. Typically, the pore size of the protein nanofibers decreased with decreasing PEO loading, and it ranged from 2 to 4 μm.

We further investigated other physical properties of the zein-based nanofabrics including the adhesion with the paper towel substrate and mechanical properties, as they are critical for their practical application. The adhesion property of the zein-based nanofabric was first compared with that of the gelatin nanofabric, as illustrated in Figs. 3(a) and 3(b). It is clear that the gelatin nanofabric (Fig. 3(a)) could be easily delaminated from the substrate. In contrast, zein-based nanofabric shows strong adhesion to the paper towel substrate, as shown in Fig. 3(b). The strong interactions between the zein-nanofabric might be due to the unique structure of the zein protein. At the same time, the zein-based nanofabric demonstrated good mechanical flexibility. As shown in Figs. 3(c) and 3(d), after several cycles of folding/unfolding, the zein-based nanofabric remained tightly attached to the substrate and maintained its structural integrity, indicating good mechanical flexibility and stability. The possible interactions between the zein nanofabrics and paper towel substrate (cellulose) are illustrated in Fig. 3(e). As shown, the functional groups of the protein such as the amide and hydroxyl groups can form hydrogen bonds with the hydroxyl groups of cellulose. In addition to the protein, PEO can also contribute to the strong adhesion to paper towel. The hydroxyl groups in both PEO and cellulose can form hydrogen bonds with each other. Thus, the zein nanofabrics show stronger adhesion to paper towel compared to gelatin nanofabrics. Figure 3(f) further compares the adhesion force with the substrate for the two types of protein nanofabrics. It is clear that the adhesion force for the zein-protein nanofabric is ~ 1 $N \cdot cm^{-1}$, which is much higher than 0.02 $N \cdot cm^{-1}$ for the gelatin nanofabric. In addition to the adhesion properties, we further studied the mechanical strength of the zein-nanofabrics (Fig. 3(g)). The tensile test results reveal that the mechanical strength of the zein-based nanofabric is higher than that of the gelatin nanofabric, but lower than that of the paper towel substrate. At

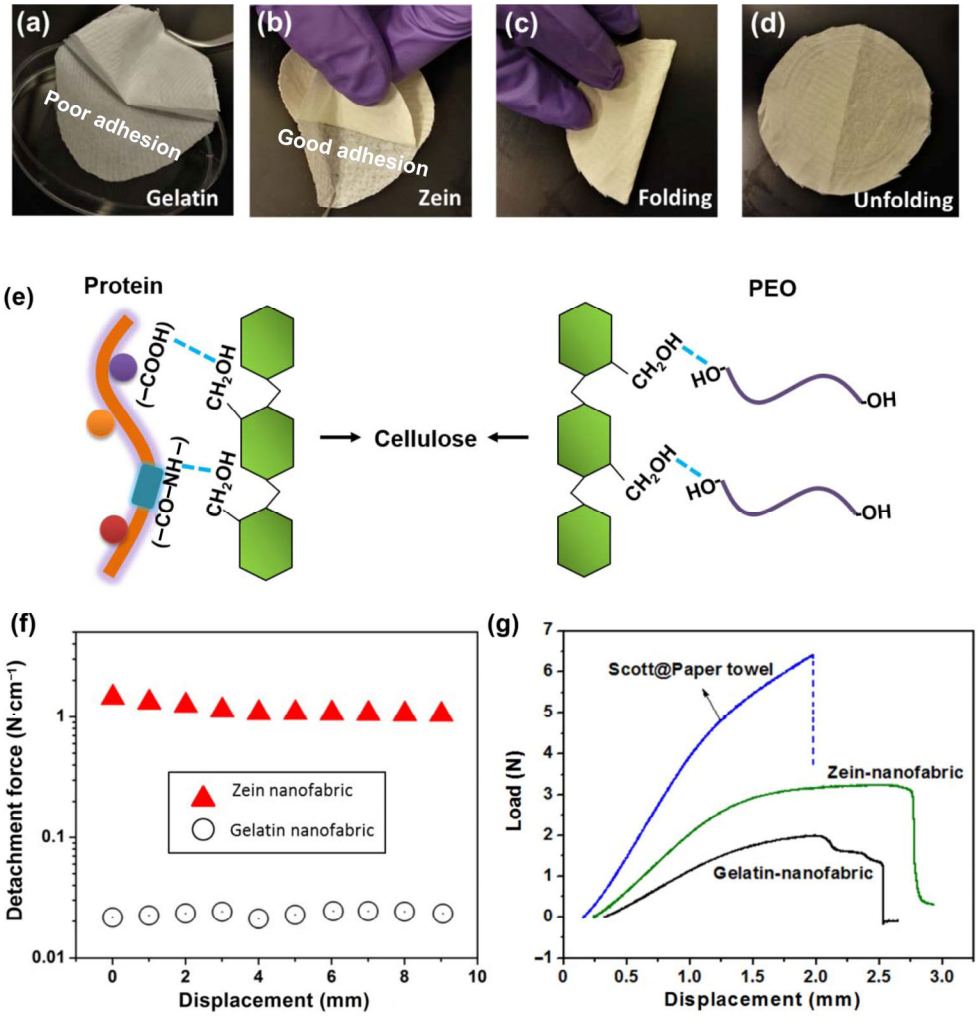

Figure 3 Mechanical and adhesion properties of the zein-based nanofabric compared to that of the gelatin nanofabric. (a) Digital photo showing the poor adhesion of the gelatin nanofabric with the paper towel substrate. (b) Digital photo showing improved adhesion of zein nanofabric with the paper towel. (c) and (d) Digital photos showing good mechanical flexibility of zein-based nanofabrics under folding and unfolding, respectively. (e) Schematic of the interactions of paper towel (cellulose) with the protein and PEO. (f) Comparison of the adhesion properties of the two protein nanofabrics, as determined by peeling-off testing. (g) Comparison of the mechanical strength of the two protein nanofabrics and the substrate, paper towel.

the same time, the zein-nanofabric could be stretched to a greater extent before its breakage, probably owing to the presence of flexible PEO that can reduce the brittleness of the protein [39]. Furthermore, as thermal stability is an important property for practical applications, we also investigated the thermal stability of the zein nanofabrics by thermogravimetric analysis (TGA) (Fig. S2 in the ESM). It was found that for all the zein nanofabrics with varying loading of PEO, they stay thermally stable until ca. 300 °C, followed by a drastic weight loss due to the degradation of zein.

The filtration performances of the zein-based nanofabrics for PM pollutants and toxic chemical gases are shown in Fig. 4. The removal efficiency for PM was first studied and the results are shown in Fig. 4(a). As illustrated, all the nanofabrics with varying loading of zein exhibit high removal efficiency of > 99.6% for particle sizes in the range of 0.3 and 10 μm. Specifically, the removal efficiency for $PM_{2.5\text{-}10}$ is almost 100% for all the zein-based air filters owing to the size effect, because the pore sizes of all nanofibers are much smaller than 10 μm (see Fig. 2(f)). Surprisingly, the nanofabric with 93% loading of zein shows the highest removal efficiency (very close to 100%) for particles of all sizes, which is believed to be a result of the optimal fiber morphology and appropriate loading of

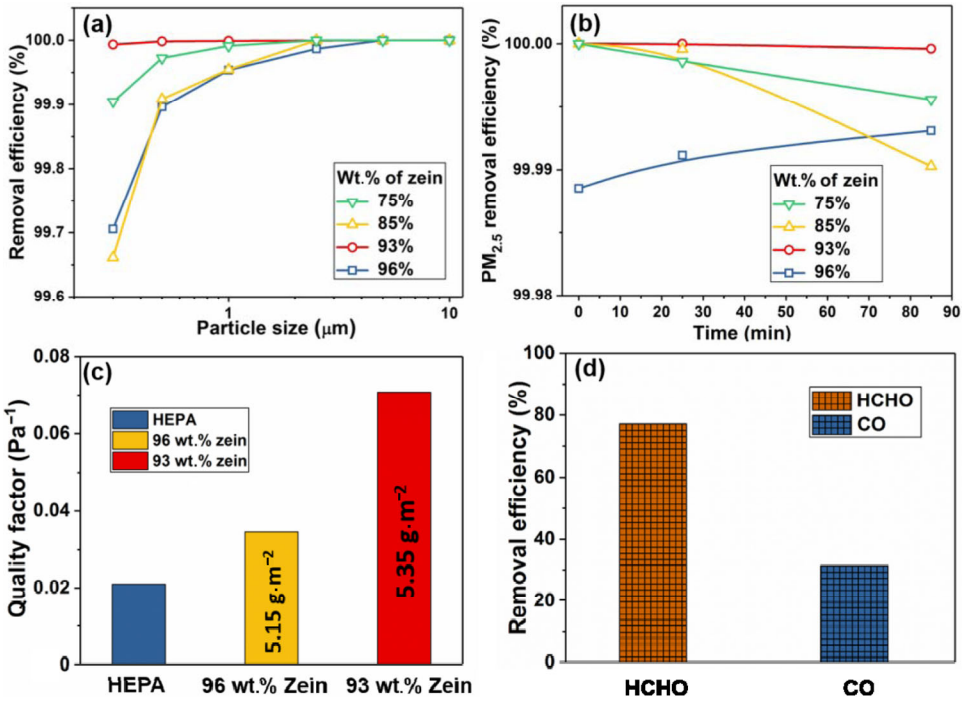

Figure 4 Filtration performance of a zein-based nanofilter. (a) Particulate removal efficiencies for PM of various particle sizes. (b) Effect of testing time on the $PM_{2.5}$ removal efficiencies. (c) Comparison of the quality factors of the commercial HEPA filter and zein-based nanofabrics filters with zein loadings of 96 wt.% and 93 wt.%. (d) Chemical removal efficiency of zein-based nanofabrics filter for formaldehyde (HCHO) and carbon monoxide (CO).

zein, which is primarily responsible for interactions with the particulates, as discussed later.

For air filtration materials, long-term performance is an important feature determining their life span, as the removal efficiency would irreversibly decrease with service time owing to their intrinsic filtration capacity. In this study, we investigated the long-term filtration performance of zein-based nanofabrics for $PM_{2.5}$ within 85 min, as shown in Fig. 4(b). For all the zein-based nanofabrics with varying zein loading, the removal efficiency was found to be above 99.98% throughout the entire testing period. At the same time, the removal efficiency of the nanofabrics decreases slightly with time due to the gradual saturation of the filtration capacity, except for the case of nanofibers with 96% loading of zein. This unique phenomenon is possibly due to the very small pore size and fiber diameter of nanofibers with 96% zein (see Fig. 2(f)), resulting in rapid saturation of the filtration capacity and the particulates significantly clog the pores of the nanofibers, which prevents the passage of the pollutants through it. It is also worth noting that for the nanofibers with 93% zein, no obvious performance decay with time was observed, which indicates that the nanofibers with 93% zein show the highest filtration capacity of all the nanofiber specimens.

For a comprehensive evaluation of the air-filtering performance, quality factor (QF) is considered by taking the removal efficiency and pressure drop into account, which can be calculated using Eq. (1) [40]

$$\mathrm{QF} = -\frac{\ln(1-\eta_{\mathrm{p}})}{\Delta P} \quad (1)$$

where, η_{p} is the removal efficiency and ΔP is the corresponding pressure drop. A desirable air filter should present high removal efficiency and low pressure drop (air resistance). Therefore, a high QF value indicates a better comprehensive filtration performance. The QF values of the zein nanofabrics in comparison with that of commercial HEPA are shown in Fig. 4(c). The QF values of zein-based nanofibers are much higher than that of commercial HEPA. Particularly, for optimized 93% zein-based nanofabrics compared to the 96% ones, with a similar areal density (5.15 and 5.35 g·m^{-2}, respectively) and pressure drop (175 and 180 Pa, respectively), the

QF value of the 93% zein-based nanofabric is much higher than that of the 96% one and is more than three times higher than that of HEPA. These results suggest that the optimized zein-based nanofabrics have great potential to serve as high-performance air filter materials that could show high removal efficiency and low pressure drop, simultaneously.

Efficient capture of toxic chemical gases is a big challenge as they are much smaller than the particulates. Previously, we investigated the chemical removal efficiencies of gelatin and soy protein and found that they exhibit excellent removal efficiencies for toxic chemicals in addition to PM of different sizes [10, 14]. In this study, we also evaluated the removal efficiency of zein-based nanofabrics for two kinds of toxic chemicals, that is, HCHO and CO. As shown in Fig. 4(d), zein-based nanofabrics (93% zein loading) show high removal efficiencies of 77% and 31% for HCHO and CO respectively, which are much higher than that of HEPA (less than 5% and 3%, respectively). It is therefore believed that the functionality and surface property of zein protein play critical roles in capturing small chemical molecules, which is governed by the interaction-based filtration mechanism, as discussed below.

To analyze the filtration mechanism of zein-based nanofabrics, we first investigated the effect of the morphology of the zein nanofibers on filtration performance. As shown in Figs. 5(a) and 5(b), the notable color change of the nanofabric surface from white to yellow after filtration is an obvious indication of the adsorption of pollutants, in particular, chemical gases such as HCHO due to the interaction between the protein and HCHO, which is consistent with the results of our previous study [10]. The SEM images shown in Figs. 5(c)–5(e) also suggest that, after filtration testing, a great number

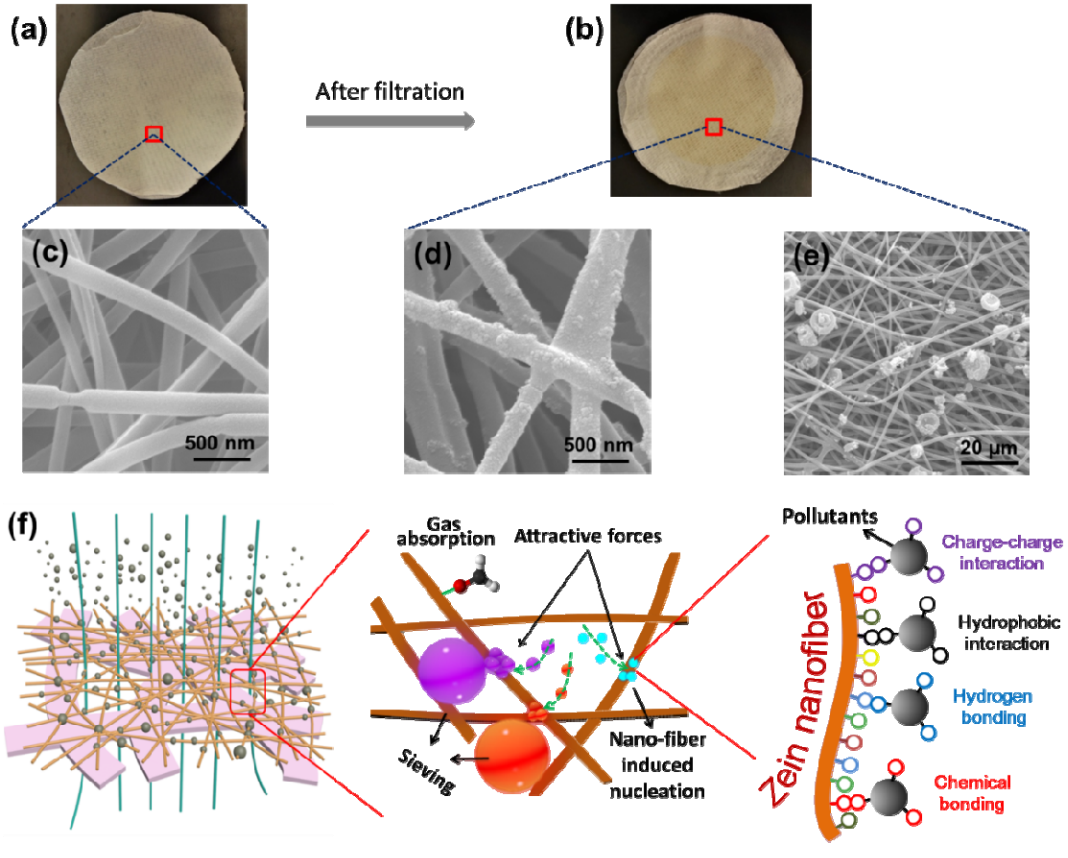

Figure 5 Filter-pollutant interactions for the zein-based nanofabrics. (a) and (b) Digital photos of the zein-based nanofabrics before and after filtration testing, respectively. (c) SEM image of the zein nano-filter before filtration. (d) and (e) SEM images of the zein nano-filter after filtration testing, showing the interactions between the filter and pollutants at different size levels. (f) Schematic of the possible filter-pollutants interactions for the zein-based nanofabrics. The functional groups from twenty kinds of amino acids provide various interactions with the pollutants, which may have different surface properties. For details, see the text.

of pollutant particles are captured on the surface of zein nanofibers. More specifically, as shown in Fig. 5(d) (for more SEM images, see Fig. S3 in the ESM), one can clearly observe that nano-sized pollutants which are much smaller than the pore size of the nanofilter are tightly captured by the protein nanofiber, and there is even a pollutant coating layer formed on the fiber surface. These SEM images indicate that there are strong interactions between the zein nanofilter and various pollutants. For large particles with sizes above the pore size, they are trapped via a simple sieving mechanism, as shown in Fig. 5(e). The possible interactions between the filter and pollutants were also investigated by FTIR (see Fig. S4 in the ESM). Probably, owing to the richness of the chemical bonds in protein, we were unable to detect any of the new peaks arising from the filter upon comparing the FTIR spectra of the sample before and after filtration.

To help understand the strong filter-pollutant interactions, we propose a structural model, as illustrated in Fig. 5(f). According to this model, the functional groups from twenty types of amino acids and the high surface area of the filter play key roles in generating strong filter-pollutant interactions. Although the compositions of the pollutants, including those of the particulates and toxic chemicals, are extremely complicated, the surface properties are basically controlled by the functional groups in their chemical structure. For smoke-based polluted air, the existence of O–H, C=O, and C–O groups in the smoke pollutants has been proven [14]. Therefore, the functional groups of zein protein may facilitate different attractive interactions with different types of pollutants, distinguished by their surface functional groups. These interactions may include electrostatic interactions, hydrophobic interactions, hydrogen bonding, and even chemical bonding. These interactions can significantly promote the absorption of especially small pollutants and toxic chemicals to the filter. For example, the zein nanofiber has functional groups including hydrophobic groups (e.g., Glycine) and charged groups (e.g., Lysine), which can provide possible hydrophobic and electrostatic interactions with the pollutants, as illustrated in Fig. 5(f). At the same time, some stronger interactions, such as chemical interactions between protein and pollutants, also occur. For example, the $–NH_2$ and –OH groups of protein are reactive to certain chemical pollutants such as HCHO, which was proven in our previous study [14]. In short, the zein nanofiber is naturally functionalized with various types of side groups, which can generate various types of interactions to efficiently remove the particulate and toxic chemical pollutants with different sizes and surface properties.

Although the protein-based nano-air-filters exhibit high filtration performances, as reported in our previous work [10], the poor water-resistance property has been the most critical drawback severely limiting their practical application, especially for the specific application as a face mask. Very different from gelatin and soy protein that have been reported previously, zein protein is dominantly hydrophobic and this is potentially beneficial for water-resistance. As revealed by Fig. S5 in the ESM, the contact angle of water on zein film is 55.4°, which is much higher than that of a film of soy protein (26.5°). We therefore demonstrate the moisture-resistance property of zein-based nanofabrics by exposing them to exhaled human breath with a high RH, ~ 100%, compared to gelatin nanofabrics (Fig. 6(a)). As shown in Fig. 6(b), the gelatin nanofabrics underwent rapid contraction and got destroyed by humidity, which suggests a very poor water-resistance property. In contrast, for zein-based nanofabrics, the high humidity level of human breath did not affect the nanofabrics and they remained tightly attached to the paper towel substrate, as shown in Fig. 6(c). Moreover, the effect of air filtration testing at a high RH level (90%) on the zein-based nanofiber morphology was characterized by SEM imaging (Figs. 6(d) and 6(e)), to demonstrate the environmental stability and humidity-resistance of the nanofabrics. The nanofiber structures are well maintained after air filtration testing in a highly humid environment, although the nanofibers show slight swelling with an increase in the fiber diameter. In a nutshell, compared to gelatin nanofabrics, the zein-based nanofabrics exhibit excellent water-resistant property and good structural stability even when exposed to an environment with a very high humidity level.

We further evaluated the air filtration performance of the filters for PM pollutants at a high RH level such as 90%. As shown in Fig. 7(a), the PM removal efficiency of zein-based nanofabrics under 90% RH remained very high above 95%, although it is found to be slightly lower than those tested under 35% RH, for removing particulates with sizes above 2.5 μm. This

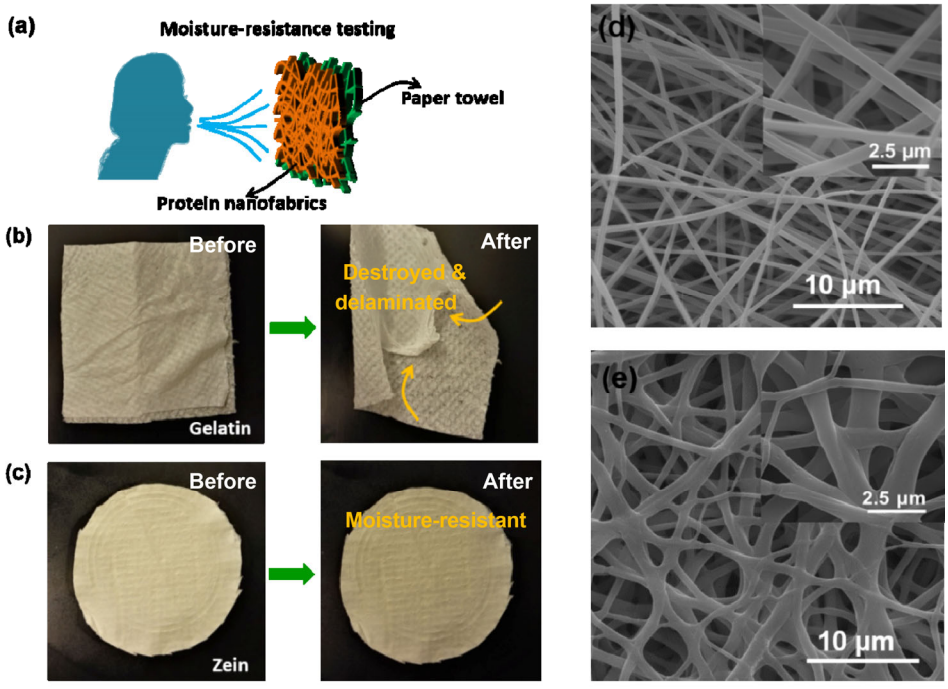

Figure 6 Study of the moisture-resistance property of zein-based nanofibers. (a) Illustration of the moisture-resistance testing by exhaling human breath toward the protein nanofabrics. (b) and (c) Digital photos showing the effect of humidity on the structural stability of gelatin nanofabrics and zein-based nanofabrics before and after exposure to human breath, respectively; SEM images of zein-based nanofabrics before (d) and after (e) filtration under 90% relative humidity (RH) condition.

indicates that the overall removal efficiency is not significantly affected by the humidity, which indicates the good environmental stability of the zein-based nanofibers. As illustrated in Fig. 7(b), with increasing testing time, the removal efficiency increases slightly for large particles, which might be ascribed to the decreased pore size owing to the gradual accumulation of particles. The pressure drop of a filter after different service times is another critical factor affecting the filter performance. Since it is highly dependent on the porous structure of the filter, the pressure drop signals the structural changes during filtration. Therefore, the evolution of pressure drop with increased filtration time at a high humid-level condition was investigated. As shown in Fig. 7(c), the pressure drop of the nanofabrics only increases from ca. 200 Pa to ca. 250 Pa after 10-min exposure to moisture, suggesting that the swelling of the fiber gives rise to higher pressure drop; however, the slightly higher pressure drop proves that the zein-based nanofibers exhibit good structural stability, and therefore, water-resistance property, which are significant advantages over other reported protein-based nano-air-filters.

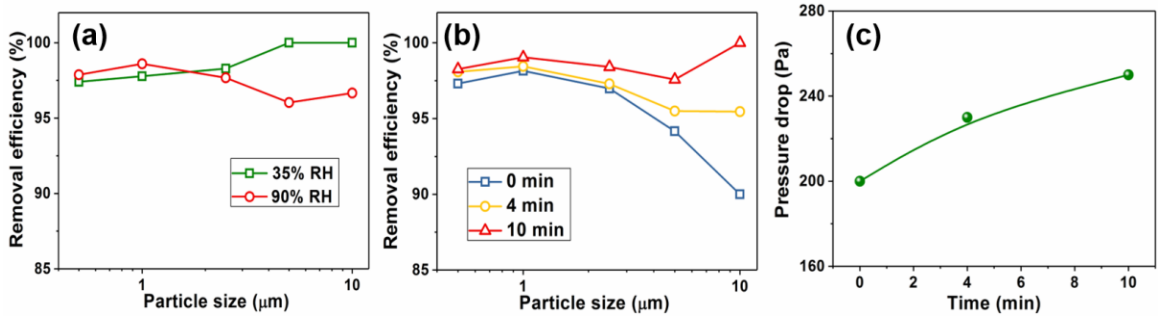

Figure 7 Air filtration performance under different humid condition. (a) Removal efficiency of the zein nanofabrics for PMs of different particle sizes at 35% and 90% RH. (b) Removal efficiency at 90% RH for different testing times. (c) Pressure drop of zein-based nanofabrics at 90% RH as a function of time.

4 Conclusions

In summary, we demonstrated high-performance filters based on zein nanofabrics with good water-resistance and mechanical properties for highly efficient and multi-functional air filtration. First, we discovered that by blending zein with a small amount of PEO, the electrospinning of zein-PEO solution to obtain nanofiber could be controlled well in terms of the processing stability, fiber diameter, and mechanically flexibility of the resultant nanofabrics. When employed as an air nanofilter, the zein-based nanofabric exhibited excellent air filtration efficiency for both PM with broad sizes ranging from 0.1 to 10 μm and toxic chemical gases such as CO and HCHO. More importantly, when compared with other nanofabrics derived from natural proteins such as gelatin, this zein-based nanofabric has several significant advantages: (1) The inherent hydrophobic property enables excellent moisture resistance and high removal efficiency of the filter in a high-humidity environment, which could not be achieved from other hydrophilic proteins; (2) the zein-protein nanofabric does not only strongly adhere to cellulose paper towel, but also improves the mechanical properties of the final filter. In summary, this study proposes a promising "green" material and processing approach for the fabrication of a multi-functional nano-filter, which is critically needed considering the increasing concerns with respect to polluted air.

Acknowledgements

This work was supported by the National Natural Science Foundation of China (No. 51373004) and Beijing Top Young Innovative Talents Program (No. 2014000026833ZK13). This work was also partly supported by USDA NIFA 2015-67021-22911.

Electronic Supplementary Material: Supplementary material (zein nanofabrics morphological statistics; SEM images, TGA curves and FTIR spectra of zein nanofabrics; wetting behavior of water on protein films) is available in the online version of this article at https://doi.org/10.1007/s12274-018-2013-0.

References

[1] Liu, C.; Hsu, P. C.; Lee, H. W.; Ye, M.; Zheng, G. Y.; Liu, N.; Li, W. Y.; Cui, Y. Transparent air filter for high-efficiency $PM_{2.5}$ capture. *Nat. Commun.* **2015**, *6*, 6205.

[2] Zhang, R. F.; Liu, C.; Hsu, P. C.; Zhang, C. F.; Liu, N.; Zhang, J. S.; Lee, H. R.; Lu, Y. Y.; Qiu, Y. C.; Chu, S. et al. Nanofiber air filters with high-temperature stability for efficient $PM_{2.5}$ removal from the pollution sources. *Nano Lett.* **2016**, *16*, 3642–3649.

[3] Liu, X. B.; Souzandeh, H.; Zheng, Y. D.; Xie, Y. J.; Zhong, W. H.; Wang, C. Soy protein isolate/bacterial cellulose composite membranes for high efficiency particulate air filtration. *Compos. Sci. Technol.* **2017**, *138*, 124–133.

[4] Zhou, Z.; Dionisio, K. L.; Verissimo, T. G.; Kerr, A. S.; Coull, B.; Arku, R. E.; Koutrakis, P.; Spengler, J. D.; Hughes, A. F.; Vallarino, J. et al. Chemical composition and sources of particle pollution in affluent and poor neighborhoods of Accra, Ghana. *Environ. Res. Lett.* **2013**, *8,* 044025.

[5] Huang, J. N.; Cao, Y. H.; Shao, J.; Peng, X. F.; Guo, Z. H. Magnetic nanocarbon adsorbents with enhanced hexavalent chromium removal: Morphology dependence of fibrillar vs. particulate structures. *Ind. Eng. Chem. Res.* **2017**, *56*, 10689–10701.

[6] Wang, C. S.; Otani, Y. Removal of nanoparticles from gas streams by fibrous filters: A review. *Ind. Eng. Chem. Res.* **2013**, *52*, 5–17.

[7] Jung, J. H.; Hwang, G. B.; Park, S. Y.; Lee, J. E.; Nho, C. W.; Lee, B. U.; Bae, G. N. Antimicrobial air filtration using airborne *Sophora Flavescens* natural-product nanoparticles. *Aerosol Sci. Technol.* **2011**, *45*, 1510–1518.

[8] Li, P.; Wang, C. Y.; Zhang, Y. Y.; Wei, F. Air filtration in the free molecular flow regime: A review of high-efficiency particulate air filters based on carbon nanotubes. *Small* **2014**, *10*, 4543–4561.

[9] Xiao, Z. G.; Li, Y. H.; Wu, X. R.; Qi, G. Y.; Li, N. B.; Zhang, K.; Wang, D. H.; Sun, X. S. Utilization of sorghum lignin to improve adhesion strength of soy protein adhesives on wood veneer. *Ind. Crop. Prod.* **2013**, *50*, 501–509.

[10] Souzandeh, H.; Wang, Y.; Zhong, W. H. "Green" nano-filters: Fine nanofibers of natural protein for high efficiency filtration of particulate pollutants and toxic gases. *RSC Adv.* **2016**, *6*, 105948–105956.

[11] Wang, C. Y.; Wu, S. Y.; Jian, M. Q.; Xie, J. R.; Xu, L. P.; Yang, X. D.; Zheng, Q. S.; Zhang, Y. Y. Silk nanofibers as high efficient and lightweight air filter. *Nano Res.* **2016**, *9*, 2590–

2597.

[12] Cheng, X. Q.; Wang, Z. X.; Jiang, X.; Li, T. X.; Lau, C. H.; Guo, Z. H.; Ma, J.; Shao, L. Towards sustainable ultrafast molecular-separation membranes: From conventional polymers to emerging materials. *Prog. Mater. Sci.* **2018**, *92*, 258–283.

[13] Fang, Q.; Zhu, M.; Yu, S. R.; Sui, G.; Yang, X. P. Studies on soy protein isolate/polyvinyl alcohol hybrid nanofiber membranes as multi-functional eco-friendly filtration materials. *Mater. Sci. Eng. B* **2016**, *214*, 1–10.

[14] Souzandeh, H.; Johnson, K. S.; Wang, Y.; Bhamidipaty, K.; Zhong, W. H. Soy-protein-based nanofabrics for highly efficient and multifunctional air filtration. *ACS Appl. Mater. Interfaces* **2016**, *8*, 20023–20031.

[15] Liu, D. G.; Chang, P. R.; Chen, M. D.; Wu, Q. L. Chitosan colloidal suspension composed of mechanically disassembled nanofibers. *J. Colloid Interface Sci.* **2011**, *354*, 6371oll.

[16] Zhang, L.; Yu, W.; Han, C.; Guo, J.; Zhang, Q. H.; Xie, H. Y.; Shao, Q.; Sun, Z. G.; Guo, Z. H. Large scaled synthesis of heterostructured electrospun TiO_2/SnO_2 nanofibers with an enhanced photocatalytic activity. *J. Electrochem. Soc.* **2017**, *164*, H651–H656.

[17] Zhang, L.; Qin, M. K.; Yu, W.; Zhang, Q. H.; Xie, H. Y.; Sun, Z. G.; Shao, Q.; Guo, X. K.; Hao, L. H.; Zheng, Y. J. et al. Heterostructured TiO_2/WO_3 nanocomposites for photocatalytic degradation of toluene under visible light. *J. Electrochem. Soc.* **2017**, *164*, H1086–H1090.

[18] Song, W. G.; Liu, D. G.; Prempeh, N.; Song, R. J. Fiber alignment and liquid crystal orientation of cellulose nanocrystals in the electrospun nanofibrous mats. *Biomacromolecules* **2017**, *18*, 3273–3279.

[19] Tian, H. F.; Xu, G. Z.; Yang, B.; Guo, G. P. Microstructure and mechanical properties of soy protein/agar blend films: Effect of composition and processing methods. *J. Food Eng.* **2011**, *107*, 21–26.

[20] Guo, G. P.; Zhang, C.; Du, Z. J.; Zou, W.; Tian, H. F.; Xiang, A. M.; Li, H. Q. Structure and property of biodegradable soy protein isolate/PBAT blends. *Ind. Crop. Prod.* **2015**, *74*, 731–736.

[21] Souzandeh, H.; Molki, B.; Zheng, M.; Beyenal, H.; Scudiero, L.; Wang, Y.; Zhong, W. H. Cross-linked protein nanofilter with antibacterial properties for multifunctional air filtration. *ACS Appl. Mater. Interfaces* **2017**, *9*, 22846–22855.

[22] Wongsasulak, S.; Tongsin, P.; Intasanta, N.; Yoovidhya, T. Effect of glycerol on solution properties governing morphology, glass transition temperature, and tensile properties of electrospun zein film. *J. Appl. Polym. Sci.* **2010**, *118*, 910–919.

[23] Shukla, R.; Cheryan, M. Zein: The industrial protein from corn. *Ind. Crop. Prod.* **2001**, *13*, 171–192.

[24] Park, J. H.; Park, S. M.; Kim, Y. H.; Oh, W.; Lee, G. W.; Karim, M. R.; Park, J. H.; Yeum, J. H. Effect of montmorillonite on wettability and microstructure properties of zein/montmorillonite nanocomposite nanofiber mats. *J. Compos. Mater.* **2013**, *47*, 251–257.

[25] Lai, H. M.; Geil, P. H.; Padua, G. W. X-ray diffraction characterization of the structure of zein-oleic acid films. *J. Appl. Polym. Sci.* **1999**, *71*, 1267–1281.

[26] Wang, C.; Wu, Y. C.; Li, Y. C.; Shao, Q.; Yan, X. R.; Han, C.; Wang, Z.; Liu, Z.; Guo, Z. H. Flame-retardant rigid polyurethane foam with a phosphorus-nitrogen single intumescent flame retardant. *Polym. Adv. Technol.* **2018**, *29*, 668–676.

[27] Li, Y. H.; Zhou, B.; Zheng, G. Q.; Liu, X. H.; Li, T. X.; Yan, C.; Cheng, C. B.; Dai, K.; Liu, C. T.; Shen, C. Y. et al. Continuously prepared highly conductive and stretchable SWNT/MWNT synergistically composited electrospun thermoplastic polyurethane yarns for wearable sensing. *J. Mater. Chem. C* **2018**, *6*, 2258–2269.

[28] Li, Y. C.; Wu, X. L.; Song, J. F.; Li, J. F.; Shao, Q.; Cao, N.; Lu, N.; Guo, Z. H. Reparation of recycled acrylonitrile-butadiene-styrene by pyromellitic dianhydride: Reparation performance evaluation and property analysis. *Polymer* **2017**, *124*, 41–47.

[29] Ma, Y. L.; Lv, L.; Guo, Y. R.; Fu, Y. J.; Shao, Q.; Wu, T. T.; Guo, S. J.; Sun, K.; Guo, X. K.; Wujcik, E. K. et al. Porous lignin based poly (acrylic acid)/organo-montmorillonite nanocomposites: Swelling behaviors and rapid removal of Pb(II) ions. *Polymer* **2017**, *128*, 12–23.

[30] Sun, K.; Xie, P. T.; Wang, Z. Y.; Su, T. M.; Shao, Q.; Ryu, J. E.; Zhang, X. H.; Guo, J.; Shankar, A.; Li, J. F. et al. Flexible polydimethylsiloxane/multi-walled carbon nanotubes membranous metacomposites with negative permittivity. *Polymer* **2017**, *125*, 50–57.

[31] Wang, C. F.; Zhao, M.; Li, J.; Yu, J. L.; Sun, S. F.; Ge, S. S.; Guo, X. K.; Xie, F.; Jiang, B.; Wujcik, E. K. et al. Silver nanoparticles/graphene oxide decorated carbon fiber synergistic reinforcement in epoxy-based composites. *Polymer* **2017**, *131*, 263–271.

[32] Wu, Z. J.; Gao, S.; Chen, L.; Jiang, D. W.; Shao, Q.; Zhang, B.; Zhai, Z. H.; Wang, C.; Zhao, M.; Ma, Y. Y. et al. Electrically insulated epoxy nanocomposites reinforced with synergistic core-shell SiO_2@MWCNTs and montmorillonite bifillers. *Macromol. Chem. Phys.* **2017**, *218*, 1700357.

[33] Zhang, K.; Li, G. H.; Feng, L. M.; Wang, N.; Guo, J.; Sun, K.;

Yu, K. X.; Zeng, J. B.; Li, T. X.; Guo, Z. H. et al. Ultralow percolation threshold and enhanced electromagnetic interference shielding in poly(L-lactide)/multi-walled carbon nanotube nanocomposites with electrically conductive segregated networks. *J. Mater. Chem. C* **2017**, *5*, 9359–9369.

[34] Wang, X. D.; Liu, X. H.; Yuan, H. Y.; Liu, H.; Liu, C. T.; Li, T. X.; Yan, C.; Yan, X. R.; Shen, C. Y.; Guo, Z. H. Non-covalently functionalized graphene strengthened poly(vinyl alcohol). *Mater. Des.* **2018**, *139*, 372–379.

[35] Souzandeh, H.; Scudiero, L.; Wang, Y.; Zhong, W. H. A Disposable multi-Functional air filter: Paper towel/protein nanofibers with gradient porous structures for capturing pollutants of broad species and sizes. *ACS Sustain. Chem. Eng.* **2017**, *5*, 6209–6217.

[36] Koombhongse, S.; Liu, W. X.; Reneker, D. H. Flat polymer ribbons and other shapes by electrospinning. *J. Polym. Sci. Pt. B-Polym. Phys.* **2001**, *39*, 2598–2606.

[37] Yao, C.; Li, X. S.; Song, T. Y. Electrospinning and crosslinking of zein nanofiber mats. *J. Appl. Polym. Sci.* **2007**, *103*, 380–385.

[38] Miyoshi, T.; Toyohara, K.; Minematsu, H. Preparation of ultrafine fibrous zein membranes via electrospinning. *Polym. Int.* **2005**, *54*, 1187–1190.

[39] Fu, X. W.; Jewel, Y.; Wang, Y.; Liu, J.; Zhong, W. H. Decoupled ion transport in a protein-based solid ion conductor. *J. Phys. Chem. Lett.* **2016**, *7*, 4304–4310.

[40] Chen, C. Y. Filtration of aerosols by fibrous media. *Chem. Rev.* **1955**, *55*, 595–623.